Nanoparticles

DOI: 10.1002/ange.201105314

Thermotropic Liquid Crystals as Templates for Anisotropic Growth of Nanoparticles

Sarmenio Saliba, Yannick Coppel, Marie-France Achard, Christophe Mingotaud, Jean-Daniel Marty, and Myrtil L. Kahn**

Control over size, shape, and composition of nanomaterials is one of the major concerns in the field of nanoscience today. This task has induced a tremendous amount of work, in which methods based on chemical or physical processes were developed to synthesize such nanosystems. Among the various strategies, organic molecules and macromolecules, exhibiting an anisotropic shape or a particular organization, have been used as templates for controlling the shape and size of inorganic materials.[1] Literature reveals particularly interesting attempts in synthesizing nanoparticles (NPs) within mesophases of liquid crystals (LCs).[2] For example, ZnSe nanomaterials have been synthesized in lyotropic systems based on amphiphilic triblock copolymers.[3] Depending on the liquid-crystalline state, quantum dots, nanodisks, or even nanowires could be obtained. Nanoporous materials (generally silica) have also been fabricated by true liquid crystal templating.[4] Whereas the large majority of such research employs lyotropic LCs, very few publications deal with the elaboration of nanomaterials within thermotropic ones.[5–8] Indeed, the development of an in situ procedure to generate NPs within an LC medium has proved to be quite a challenging task. Most studies involve the in situ reduction of metal precursors through oxidation of the LC medium in order to obtain the desired NPs. For example, the formation of CuCl nanostructures inside a mixture of an ionic liquid and a derivative of ascorbic acid has been reported. This approach resulted in the formation of CuCl nanoplatelets with a relatively uniform thickness of about 220 nm and in-plane sizes of 5–50 μm.[5a–c] Glass-forming liquid-crystalline materials acting as a reducing agent were also used to obtain Au NPs, the size and shape of which depended on both the amount of precursor content and the LC state.[5d] Isotropic NPs of gold or silver have also been synthesized by heating LC materials doped with the corresponding metal salts.[6] In other cases sputtering[7] or electrodeposition[8] techniques were used to form NPs in thermotropic systems. However, none of the examples above have shown a direct relation between the structure of the LCs and the morphology of the synthesized NPs. For the few examples that report an anisotropic growth, structures in most cases have been outside the nanometer range. To improve such results, we suggest that three criteria should be fulfilled in order to tailor the NP morphology using an LC phase; 1) the chemical reaction leading to the NPs should not disrupt the LC organization. Thus the LC molecules should not play the role of reactants (side products should be avoided as much as possible throughout the NP formation). 2) Interactions between the LC molecules, the NP precursor, and eventually the synthesized NPs should favor the templating effect of the LC phase. 3) The use of relatively high viscosity LCs should prevent a fast disruption of the organization during the NP formation.

We have previously described a very simple organometallic method for the formation of zinc oxide NPs with only cyclohexane as a side product.[9] Such a reaction may fulfill the first criterion. ZnO was therefore chosen as the inorganic material for this study. The use of LC compounds that have an oligomeric or a polymeric structure may fulfill the last two criteria. Indeed, such compounds may contain various functionalities (e.g. amine groups[9b,10]) that favor interactions between the LCs and the ZnO precursors/ZnO NPs). We have chosen to work with two different types of LCs that differ by their type of backbone. A first type involves a trisamine molecule (tris(2-aminoethyl)amine, TREN) as the backbone and a second type, a hyperbranched polyamidoamine core (HYPAM). Ideally, the target LC should exhibit a mesophase (i.e. nematic phase) close to or at ambient temperature to avoid any precursor thermal breakdown before NPs are produced. Thus, concerning the previously mentioned backbones, we chose to branch a phenylbenzoate mesogenic derivative, namely the 4-(4-acryloyloxybutyloxy)-phenyl-4′-(methoxy) benzoate (see S1A in the Supporting Information for characterization details). Figure 1 shows the envisaged LC molecules.

Differential scanning calorimetry (DSC) demonstrates that both compounds present a glass transition (as expected for oligomeric or polymeric structures) below 0 °C and a LC isotropic phase transition around room temperature (see sections S2 and S3 in the Supporting Information). Polarized optical microscopy (POM) and small-angle X-ray diffraction (SAXS) experiments have shown that TREN-LC and HYPAM-LC present a nematic phase below the clearing temperature (see sections S2 and S3 in the Supporting Information). The syntheses of the ZnO NPs in the two thermotropic LCs were performed as follows: in a typical

[*] Dr. S. Saliba, Dr. Y. Coppel, Dr. M. L. Kahn
Laboratoire de Chimie de Coordination, CNRS UPR 8241, Université de Toulouse
205, route de Narbonne, 31077 Toulouse Cedex 04 (France)
E-mail: myrtil.kahn@lcc-toulouse.fr
Dr. S. Saliba, Dr. C. Mingotaud, Dr. J.-D. Marty
Laboratoire IMRCP, CNRS UMR 5623, Université de Toulouse
118, route de Narbonne, 31062 Toulouse Cedex 09 (France)
E-mail: marty@chimie.ups-tlse.fr
Dr. M.-F. Achard
Centre de Recherche Paul Pascal
115 Avenue Schweitzer, 33600, Pessac (France)

Supporting information for this article is available on the WWW under http://dx.doi.org/10.1002/anie.201105314.

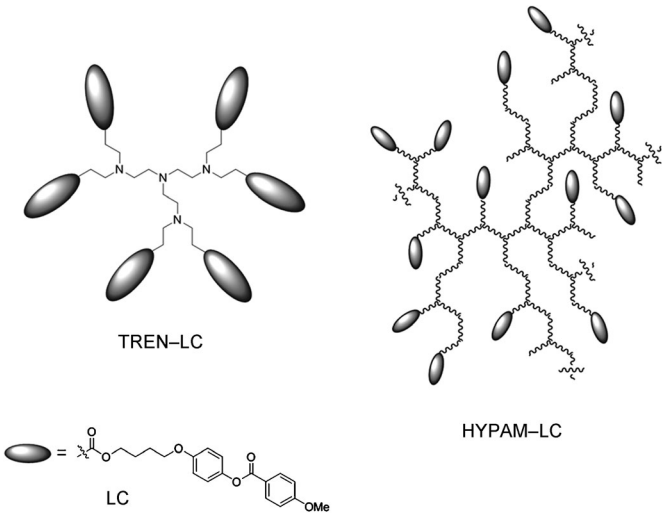

Figure 1. Schematic representation of the LC compounds used herein.

experiment, the organometallic precursor, $[Zn(C_6H_{11})_2]$ (noted as $[Zn(Cy)_2]$), was added to a solution of either TREN-LC or HYPAM-LC in anhydrous THF. Mixing of the LC with the ZnO precursor in a solvent at the pre-hydrolysis stage ensured a good material homogeneity. After evaporation of the THF under vacuum, the reaction vial was removed from inert conditions, closed, immersed in a bath at the desired temperature, and then opened to the atmosphere. A few hours after treatment, the resulting products became luminescent (under UV irradiation) in the yellow region of the visible spectrum. This is a well-known characteristic of ZnO NPs, thus confirming their presence. Figure 2 shows typical TEM micrographs of the ZnO nanostructures, the morphologies of which depend on the experimental conditions.

In isotropic conditions, hydrolysis of the $[Zn(Cy)_2]$ precursor led to isotropic NPs, as shown in Figure 2a and b.

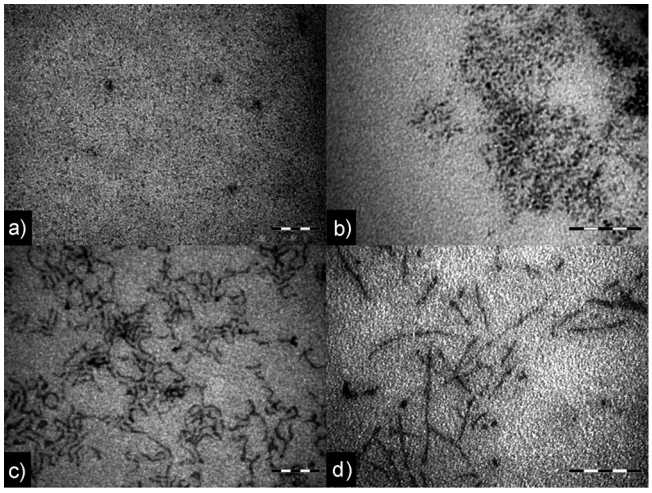

Figure 2. TEM micrographs of ZnO NPs synthesized under various conditions: a) in TREN-LC at 30 °C (scale bar: 200 nm); b) in HYPAM-LC at 45 °C (scale bar: 50 nm); c) in TREN-LC at 5 °C (scale bar: 50 nm), and d) in HYPAM-LC at 5 °C (scale bar: 50 nm).

More precisely, pure TREN-LC and HYPAM-LC are isotropic at 30 °C and 45 °C, respectively. At these given temperatures, growth control could be achieved: the average size of the NPs is around 5.4(0.7) nm in the case of TREN-LC and 2.7(0.3) nm for HYPAM-LC. When the experiments were performed in the nematic phase of the LC compound (i.e. at lower temperatures), anisotropic ZnO structures were obtained. As shown in Figure 2c and d, nanoworm-like or nanowire-like structures were grown in TREN-LC and HYPAM-LC, respectively. Nanoworms have an average width of (2.5 ± 0.2) nm and nanowires (2.7 ± 0.4) nm. Polydisperse lengths that vary from a few nanometers up to around 100 nm were observed when TREN-LC was used, while lengths from around 10 to 200 nm were obtained with HYPAM-LC. High-resolution transmission electron microscopy (HRTEM) performed on the as-synthesized nanostructures clearly showed two orientations. Indeed, some nanostructures are small enough to present their *c* axis perpendicular to the grid. Figure 3a corresponds to the observation

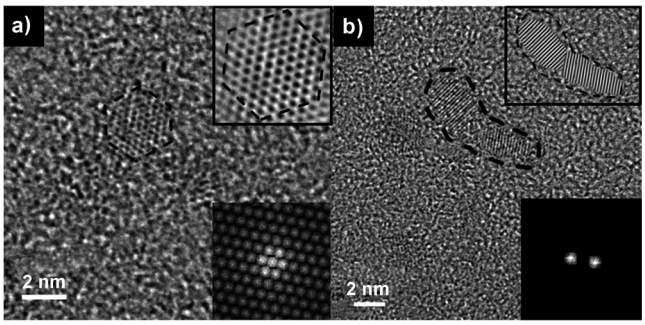

Figure 3. a), b) High-resolution TEM micrographs of a TREN-LC/ZnO nanocomposite (synthesized at 5 °C) showing two crystal orientations perpendicular and parallel to the *z* plane, respectively. Insets correspond to the filtered Fourier transform images (bottom) and the inverse Fourier transform images (top), allowing a very good reconstruction of the experimental HRTEM images.

of a ZnO with the *c* axis perpendicular to the grid (inter-atomic distance equal to 0.320 nm within the accuracy of the measurement corresponding to the shorter distance in the *ab* plane associated with the Zn–Zn distance). Whereas Figure 3b is a micrograph of a ZnO with its *c* axis parallel to the grid (inter-atomic distance equal to 0.265 nm within the accuracy of the measurement corresponding to the shorter distance along the *c* axis associated with the Zn–O distance). In the latter, we observed a disappearance of the diffracting planes at the point of curvature, which can be associated with defects in the atomic packing. This experiment puts the hexagonal wurtzite structure ($a = b = 3.2$ Å and $c = 5.2$ Å, space group: *P6mc*) in evidence and demonstrates that the anisotropic growth proceeds along the *c* axis. The sample was further analyzed by energy-dispersive X-ray spectroscopy (EDX) and the results confirmed the presence of elemental zinc.

Clearly and for the first time, the use of thermotropic LC molecules of increasing size allows the growth control of ZnO

nanoobjects. Importantly, when the thermotropic LC molecules are used in their nematic phase state, anisotropic ZnO nanoobjects are formed, the aspect ratio and the straightness of which increases when using HYPAM-LC instead of TREN-LC. Therefore, control over the shape and size of ZnO NPs can be achieved by selecting the right LC compound and the LC phase, in which the NP synthesis is performed.

To better understand such LC/ZnO nanocomposites, we analyzed the nature of possible interactions between the LC compounds and the ZnO nanocrystals. Taking TREN-LC as an example, solid-state ^{13}C NMR studies were performed at 22 °C on 1) the TREN-LC molecule alone, 2) the TREN-LC/$[Zn(Cy)_2]$ mixture, and 3) the TREN-LC/ZnO NPs nanocomposites. For the TREN-LC molecule alone, broad and complex signals were observed, confirming that TREN-LC is spatially heterogenous (see section S2 in the Supporting Information). Addition of $[Zn(Cy)_2]$ (pre-hydrolysis state) has an effect on the line shape of NMR signals, a behavior that is even more pronounced upon NP formation. Briefly, the carbonyl signals ($\delta^{13}C$ between 150 to 180 ppm) and the methylene signals in the α position with respect to amine functionalities ($\delta^{13}C$ between 40 to 45 ppm), show an important broadening in the presence of NPs. On the contrary, some aromatic ($\delta^{13}C$ between 110 to 130 ppm), the methoxy ($\delta^{13}C = 56$ ppm), and the $OCH_2CH_2CH_2CH_2O$ signals ($\delta^{13}C = 26$ ppm) are sharpened. This result can be tentatively explained by an interaction of TREN-LC molecules with ZnO NPs through the nitrogen atoms and carbonyl functions. This interaction increases the local spatial heterogeneity for these atoms close to the ZnO surface (signal broadening). The atoms farther from the surface can experience a more homogeneous environment or an increase in mobility (signal sharpening). The multiple interactions with nitrogen atoms and carbonyl groups may be used to explain the stability of ZnO in such LC hosts. Whatever the exact nature may be, these experiments demonstrated that we have interactions of the LC with the ZnO precursor and the ZnO NPs, as expected.

DSC, POM, and SAXS experiments were also carried out to investigate the LC behavior of the newly synthesized LC/ZnO nanocomposites. Figure 4a is a thermogram profile for TREN-LC/ZnO that presents a thermodynamically stable mesophase, therefore visible on both heating and cooling ramps. The LC transition peak occurs at 37 °C and a change in heat capacity linked to a T_g could be observed at −1 °C. Since pure TREN-LC exhibits the LC state between −22.0 and 9.6 °C (see S2 in the Supporting Information), we can clearly conclude that the presence of ZnO NPs shifts the mesophase temperature window towards higher temperatures. The thermo-optical behavior observed between crossed polarizers was in agreement with the previously mentioned DSC results. In other words, birefringent textures corresponding to a nematic phase could be observed within the mesophase temperature range (Figure 4b). This texture then turns darker as it approaches the isotropic state. In addition, SAXS measurements showed diffuse rings at $d = 4.5$ Å, corresponding to the inter-mesogenic distance in a nematic LC phase (Figure 4c). Similar results were obtained for HYPAM-LC/ZnO composites (section S3 in the Supporting Information).

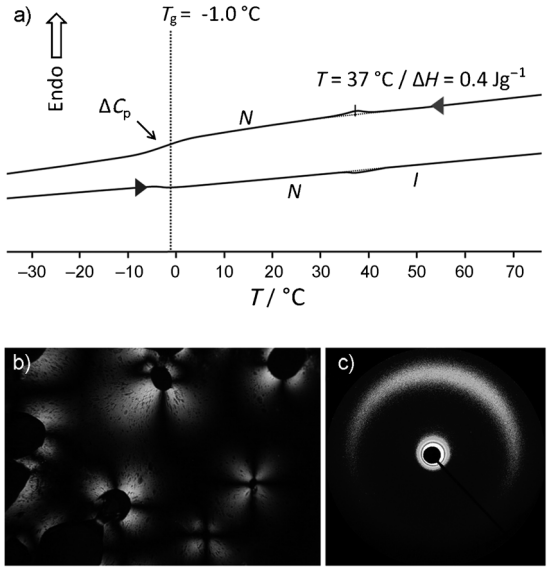

Figure 4. a) DSC thermogram for TREN-LC/ZnO at a rate of 5 °C min^{-1}; b) POM image for TREN-LC/ZnO at 20 °C, and c) a typical SAXS pattern for the nanocomposite.

Such experiments demonstrate that the final composite presents a nematic LC phase. Due to the high reactivity of the ZnO precursor, monitoring of the LC state before ZnO formation cannot be performed. However, the previous data showed that the nematic state does exist in most stages of the reaction, the most important being at reaction completion.

The results reported above allow us to conclude that ZnO nano-objects can be fabricated in thermotropic LCs by a straightforward organometallic method and that the use of a nematic phase favors the well-sought-after anisotropic growth of metal oxide NPs. Moreover, a direct correlation between the structural characteristics of the LC and the morphology of the nanostructures was demonstrated. The novel LC/NP composites present, at the same time, LC properties and optical properties originating from ZnO. This in situ strategy paves the way for new LC/NP composites of controllable and stable properties. Influence of more "complex" LC phases on NP size and shape is currently under study.

Experimental Section

Materials, characterization techniques, and methods are described in the Supporting Information. The synthesis of liquid crystal molecules was adapted from literature,[11] whereas the synthesis of the HYPAM core was carried out following previously published work by our group.[12]

Received: July 28, 2011
Revised: September 26, 2011
Published online: October 17, 2011

Keywords: anisotropic growth · liquid crystals · nanoparticles · organometallic chemistry · zinc oxide

[1] a) S. Mann, *Nat. Mater.* **2009**, *8*, 781 – 792; b) C. Sanchez, P. Belleville, M. Popall, L. Nicole, *Chem. Soc. Rev.* **2011**, *40*, 696 – 753; c) H. B. Qiu, S. N. Che, *Chem. Soc. Rev.* **2011**, *40*, 1259 – 1268; d) J. Y. Yuan, Y. Y. Xu, A. H. E. Müller, *Chem. Soc. Rev.* **2011**, *40*, 640 – 655.

[2] T. Hegmann, H. Qi, V. M. Marx, *J. Inorg. Organomet. Polym. Mater.* **2007**, *17*, 483 – 508.

[3] a) G. N. Karanikolos, P. Alexandridis, R. Mallory, A. Petrou, T. J. Mountziaris, *Nanotechnology* **2005**, *16*, 2372 – 2380; b) G. N. Karanikolos, N. L. Law, R. Mallory, A. Petrou, P. Alexandridis, T. J. Mountziaris, *Nanotechnology* **2006**, *17*, 3121 – 3128.

[4] M. Groenewolt, M. Antonietti, S. Polarz, *Langmuir* **2004**, *20*, 7811 – 7819.

[5] a) A. Taubert, *Angew. Chem.* **2004**, *116*, 5494 – 5496; *Angew. Chem. Int. Ed.* **2004**, *43*, 5380 – 5382; b) A. Taubert, P. Steiner, A. Mantion, *J. Phys. Chem. B* **2005**, *109*, 15542 – 15547; c) A. Taubert, C. Palivan, O. Casse, F. Gozzo, B. Schmitt, *J. Phys. Chem. C* **2007**, *111*, 4077 – 4082; d) V. A. Mallia, P. K. Vemula, G. John, A. Kumar, P. M. Ajayan, *Angew. Chem.* **2007**, *119*, 3333 – 3338; *Angew. Chem. Int. Ed.* **2007**, *46*, 3269 – 3274.

[6] a) I. Gascon, J. D. Marty, T. Gharsa, C. Mingotaud, *Chem. Mater.* **2005**, *17*, 5228 – 5230; b) P. K. S. Antharjanam, E. Prasad, *New J. Chem.* **2010**, *34*, 420 – 425.

[7] H. Yoshida, K. Kawamoto, H. Kubo, T. Tsuda, A. Fujii, S. Kuwabata, M. Ozaki, *Adv. Mater.* **2010**, *22*, 622 – 626.

[8] W. Dobbs, J. M. Suisse, L. Douce, R. Welter, *Angew. Chem.* **2006**, *118*, 4285 – 4288; *Angew. Chem. Int. Ed.* **2006**, *45*, 4179 – 4182.

[9] a) M. L. Kahn, M. Monge, E. Snoeck, A. Maisonnat, B. Chaudret, *Small* **2005**, *1*, 221 – 224; b) M. Monge, M. L. Kahn, A. Maisonnat, B. Chaudret, *Angew. Chem.* **2003**, *115*, 5479 – 5482; *Angew. Chem. Int. Ed.* **2003**, *42*, 5321 – 5324.

[10] M. L. Kahn, M. Monge, V. Colliere, F. Senocq, A. Maisonnat, B. Chaudret, *Adv. Funct. Mater.* **2005**, *15*, 458 – 468.

[11] J. D. Marty, M. Mauzac, C. Fournier, I. Rico-Lattes, A. Lattes, *Liq. Cryst.* **2002**, *29*, 529 – 536.

[12] a) S. Saliba, C. Valverde Serrano, J. Keilitz, M. L. Kahn, C. Mingotaud, R. Haag, J. D. Marty, *Chem. Mater.* **2010**, *22*, 6301 – 6309; b) N. Pérignon, J. D. Marty, A. F. Mingotaud, M. Dumont, I. Rico-Lattes, C. Mingotaud, *Macromolecules* **2007**, *40*, 3034 – 3041.

